Ultra-High-Pressure Ion Chromatography with Suppressed Conductivity Detection at 70 MPa Using Columns Packed with 2.5 µm Anion-Exchange Particles

Wouters, Sam; Dores-Sousa, Jose Luis; Pohl, Christopher A.; Eeltink, Sebastiaan

Published in:
Analytical Chemistry

DOI:
10.1021/acs.analchem.9b03283

Publication date:
2019

Document Version:
Accepted author manuscript

Ultra-high-pressure ion chromatography with suppressed conductivity detection at 70 MPa using columns packed with 2.5 µm anion-exchange particles

Sam Wouters[1], José Luís Dores-Sousa[1], Yan Liu[2], Christopher A. Pohl[2], Sebastiaan Eeltink[1,*]

[1]Vrije Universiteit Brussel (VUB), Department of Chemical Engineering, Brussels, Belgium

[2]Thermo Fisher Scientific, Sunnyvale, USA

(*) corresponding author

Pleinlaan 2, B-1050, Brussels, Belgium

Tel.: +32 (0)2 629 3324, Fax: +32 (0)2 629 3248

E-mail: sebastiaan.eeltink@vub.be

ABSTRACT

The use of ultra-high pressures in combination with columns packed with 2.5 µm microporous and super-macroporous (perfusive) stationary phase particles coated with nanobeads has been successfully explored in ion chromatography with on-line eluent generation and suppressed conductivity detection. Isocratic separations of inorganic anions and organic acids yielding reduced plate heights as low as 2.1 were achieved, corresponding to efficiencies up to 190,000 plates/m, using an optimized system configuration with respect to injection parameters, considering volume and mass loadability, and extra-column dispersion. Viscous-heating effects have been assessed for PEEK-lined stainless steel-columns operated at 70 MPa, and effects of thermal gradients on separation efficiency and retention are demonstrated. Whereas the PEEK-lined column hardware acts to some extent as an insulator, a 10% increase in plate number could be obtained when applying a still-air column oven configuration. In forced-air mode, an increase in retention was observed for polyvalent ions. Finally, the kinetic performance limits of ultra-high-pressure ion chromatography applying 2.5 µm particle-packed columns operated at 70 MPa were compared to conventional ion-chromatography technology using columns packed with 4 µm particles operated at a maximum pressure of 35 MPa. Downscaling the particle size and increasing the operating pressure led to a maximum time gain with a factor of 3.4, without compromising separation efficiency (N = 10,000).

***Keywords**:* Anion-exchange chromatography, latex-agglomerated stationary phase, kinetic performance limit, band broadening, viscous heating

INTRODUCTION

A seminal paper in the field of ion chromatography (IC) was published by Small and coworkers in 1975 in Analytical Chemistry, showing for the first time the concept of ion-exchange chromatography in combination with suppressed conductivity detection.[1] Due to development of dedicated hardware compatible with corrosive solvents and the availability of a broad range of stationary phase chemistries and architectures providing unique selectivites,[2-4] ion chromatography has emerged as key enabling technology for the analysis of ionic and ionizable analytes. Trends in the development of such dedicated hardware for ion analysis have been recently reviewed by Haddad *et al*.[5] The separation capabilities of IC complement those of more classical liquid chromatography (LC) modes, and examples of key IC applications include the screening for toxic substances in drinking and surface water (*e.g.* glyphosate, perchlorate, arsenate),[6-8] quality control in the food and beverages industry (*e.g.*, presence and levels of sulfite, organic acids, amines),[9,10] monitoring of levels of corrosives (*e.g.*, sulfate, chloride), and corrosion inhibitors in cooling circuits of (nuclear) power plants to safeguard operation. In the latter field of application, the samples are usually complex aqueous matrices containing ethanolamine, morpholine, or ammonium, with lithium hydroxide, and boric acid, acting as corrosion inhibitors, pH regulators, and neutron absorbers.[11,12]

With respect to the kinetic performance, *i.e.* separation efficiency *versus* analysis time, which is to a large extent affected by column-length / particle-size combination and pressure capabilities, ion chromatography is still in its infancies compared to conventional ultra-high-pressure (UHP-)LC technology. Back in the late 1990's Jorgenson *et al.* introduced the concept of UHPLC, when this group described the use of columns packed with 1.5 µm particles and applying pressures as high as 410 MPa.[13] This later led to the introduction of ultra-high-performance liquid chromatography instrumentation in 2004, capable of delivering inlet pressures of 100 MPa, allowing for the use of 1.7 µm particles.[14] Currently, the state-of-the-art UHPLC system allows delivery of 150 MPa and columns packed with sub-2 µm particles are common practice.[15] The maximum operating pressure for IC is currently limited

to 35 MPa. This limit is mainly a consequence of the use of corrosive and acidic eluents, placing stringent demands on materials selection, limiting manufacturers to the use of engineering thermoplastics such as poly(ether-etherketone) and the application of membrane technology in the eluent generator, positioned in the high-pressure flow path, downstream of the pump.[5,17] For ion chromatography (applying corrosive mobile phases), 4 µm particle-packed columns constitute the current state-of-the-art, which limits to some extent the analysis-time reduction possibilities.

The current contribution discusses the potential of a prototype ultra-high pressure IC (UHPIC) system with an operating pressure of maximum 70 MPa, in combination with PEEK-lined stainless-steel column hardware packed at 150 MPa with sulfonated 2.5 µm microporous or 2.5 µm super-macroporous particles coated with 40 nm latex particles, providing anion-exchange functionalities with different capacity and selectivity. The importance of system optimization to minimize dispersion is illustrated. Furthermore, axial- and radial-temperature profiles induced by frictional heating have been recorded and effects on retention and efficiency have been assessed at near isothermal and adiabatic conditions. Finally, the kinetic performance limits of UHPIC are compared with that of conventional IC, and the method speed-up potential has been investigated.

EXPERIMENTAL SECTION

Column Manufacturing. Column hardware for ultra-high-pressure experiments comprised of a PEEK-lined stainless-steel housing (2.0 mm i.d. × 100 mm and 150 mm) and was obtained from Idex HS (Oak Harbor, USA). Columns were packed with 2.5 µm crosslinked polymeric particles applying a high-pressure slurry packing approach.[18,19] Aqueous slurries containing surfactant and 5-15 wt% of particles were prepared and introduced in a slurry reservoir after vigorous shaking for 10 min. Using a Haskel pump the inlet pressure was gradually ramped up during 1 min to reach a packing pressure of 100 MPa for 100 mm columns and 150 MPa for 150 mm long column formats to maintain the packing flow rate. After

packing was completed, the pressure was slowly released over the course of 15 min, and the inlet end-fitting was fitted onto the column. A post-functionalization step was carried out, in which an aqueous latex containing 40 nm nanoparticles was pumped through the column until the pressure stabilizes (the point of saturation). A layer of nanoparticles is electrostatically bonded to the accessible surface of the beads, providing the final anion-exchange selectivity. Columns packed 2.5 µm super-macroporous particles (SMP) with a pore diameter of 1500 Å were coated with nanobeads carrying a triethylamine-based chemistry. Columns packed with 2.5 µm microporous particles (MiP) with a sub-20 Å pore diameter were coated with nanobeads carrying a dimethylethanolamine-based chemistry. Next, the columns were rinsed at a constant flow rate and applying a 2 h gradient starting with ACN and having a final mobile-phase composition of 30 mM potassium hydroxide, to flush out remaining surfactant and excess of nanobeads. Scanning-electron micrographs of resin particles have been made using a FEG-SEM (Jeol, Tokio, Japan). Particle-size distributions were determined via coulter-counter measurements (Multisizer 3, Beckman Coulter, Brea, USA).

Chromatographic System. Ultra-high-pressure experiments were conducted using a prototype instrument based on a ICS5000 ion chromatography system (Thermo Fisher Scientific, Sunnyvale, USA) combined with a quaternary low-pressure gradient pump capable of delivering 105 MPa (Vanquish Flex, Thermo Fisher Scientific, Germering, Germany), and a Vanquish column-oven compartment fitted with a 6-port high-pressure injection valve with ceramic rotor. The full-loop injection mode was utilized, varying loop sizes between 0.5 and 8 µL by changing the tubing i.d. and length. An experimental high-pressure electrolytic potassium hydroxide (KOH) eluent generator and degasser was used, based on the standard stacked-membrane high-capacity eluent generator. The high-pressure water flow path from the pump to eluent generator was established using a length of 100 µm i.d. metal-free Viper tubing (Thermo Fisher Scientific). 100 µm i.d. PEEK-lined stainless steel MarvelXACT tubing (Idex HS) was used to establish the high-pressure hydroxide flow path from the eluent generator to the injector (300 mm long tubing) and from the injector to the column (250 mm

long tubing), respectively, and a 65 µm i.d. × 220 mm long PEEK Viper tubing was used to establish the low-pressure hydroxide flow path from column to suppressor. Eluent suppression was performed using an ERS500 electrolytic anion suppressor with an internal volume of 15 µL (2.5 mm wide × 75 mm long) and a prototype device with an internal volume of 7.5 µL (1.0 mm wide × 75 mm long). Both devices were operated in 'external water mode', applied using the ICS5000 analytical pump, to ensure proper sweep-out of electrolysis products and byproducts. Conductivity detection was performed using the standard analytical-scale detector featuring 250 µm i.d. × 300 mm inlet tubing with preheater and a cell volume of 0.7 µL, and a prototype detector fitted with 100 µm i.d. × 200 mm inlet tubing, featuring a 20-nL flow cell (flow cell taken from a standard capillary IC detector). Detection was performed at 10 Hz and the temperature of the detector cell was set at 35°C. Chromeleon 7.2 chromatography data system software (Thermo Fisher Scientific) was used for instrument control and data processing.

Test Conditions and Evaluation. Experiments were performed in isocratic mode by injecting mixtures of small inorganic ions and organic acids (fluoride, chlorite, chloride, sulfate, thiosulfate, bromide, nitrite, nitrate, succinate, and oxalate) with analyte concentrations ranging between 1-50 µg/mL. The concentration of the sample solution and KOH mobile phase eluent concentration was adjusted to match the capacity of the stationary phase resin, *i.e.*, 35 mM KOH for the high-capacity columns packed with SMP resin and 23 mM for the low-capacity columns packed with MiP resin. Plate numbers were determined based on the retention time and the peak width at half height. No corrections were made for extra-column dispersion contributions. Kinetic plots were constructed using the mathematical approach described by Desmet *et al*.[20,21] On-column temperature profiles were recorded using copper-constantan (T-type) thermocouples attached to the end-fittings of the columns. Temperature data read-out was performed using a NI9211 CompactDAQ module (National Instruments, Austin, USA) in conjunction with SignalExpress (National Instruments) software. Conventional IC experiments were performed using a 2 mm i.d. × 250 mm column packed with 4 µm super-

macroporous beads functionalized with 65 nm nanobeads (AS16) obtained from Thermo Fisher Scientific.

RESULTS AND DISCUSSION

System design and optimization. A schematic overview of the system configuration utilized to conduct the ultra-high-pressure experiments is depicted in Fig. S1 in the Supporting Information (SI). The application of ultra-high pressure in IC leads to maximally 2.4% compression of the aqueous eluent and significant adiabatic heating of the mobile phase affecting the fluid density when operating the pump at 70 MPa. To ensure accurate flow delivery, a UHPLC pump was utilized that accounts for solvent compressibility and delivers solvent once the thermal effects have reached an equilibrium and the piston speed is adjusted, taking heat dissipation into account.[22] A prototype on-line eluent generator, based on the single-membrane design originally proposed by Dasgupta *et al.*,[23,24] as well as a prototype degasser, both with an extended pressure resistance up to 70 MPa, were integrated in the high-pressure flow path. The high-pressure degasser utilizes a Teflon AF supported membrane with a 19 cm flow path. Fig. 1A shows the novel column hardware for ultra-high-pressure operation compatible with corrosive mobile phases. To establish a metal-free fluidic path, PEEK-lined SS tubing was utilized for the column hardware, and the end-fittings accommodate an insert featuring a fitting seat and an integrated PEEK frit. SEM images of the microporous (MiP) and super-macroporous (SMP) particles having a mode particle diameter of 2.5 µm are displayed in different magnifications in Fig. 1B. Coulter-counter measurements confirmed that MiP resin had a much narrower particle-size distribution (D_{10}: 1.89) than the SMP resin (D_{10}: 2.44). Note that the anion-exchange chemistry in these columns is induced by a nanobead coating. The SEM images in Fig. 1C shows close-ups of the bare particles in comparison with the stationary-phase particles covered with a homogeneous layer of nanobeads, that were extracted from the column after operating at 70 MPa.

Fig. 2A depicts a UHPIC separation of small inorganic anions obtained on a 150 mm long column packed with 2.5 µm super-macroporous particles coated with 40 nm nanobeads, operated at the optimum van Deemter flow rate (u_{opt}) using the optimized system configuration (see below). Applying a mobile-phase ionic strength of 35 mM KOH, the retention factors (k) ranged between 0.1 and 4.6 and the corresponding volumetric peak variances (σ_v^2-values) ranged between 6 and 116 µL^2, yielding reduced plate heights of 3 for ions with $k \geq 1.4$. As a reference, in a conventional IC system, applying a 2 mm i.d. × 250 mm long column packed with 4 µm particles, the peak variances for the same k-range were a factor 4-6 larger. When operating the UHPIC column at maximum system pressure close to 70 MPa, the separation was completed in only 7 min while baseline resolution was maintained, see Fig. 2B. Although the column is then operated at a flow rate well above the optimum van Deemter flow velocity, only a 5% increase in peak variance was observed, which can be attributed to the limited resistance to mass transfer due to the perfusive character of this stationary phase architecture utilized.

Preserving these high separation efficiencies provided by ultra-high-pressure IC technology is extremely challenging, due to the nature of the instrument where the extra-column peak variance ($\sigma_{v,ext}^2$) is defined as:

$$\sigma_{v,ext}^2 = \sigma_{v,inj}^2 + \sigma_{v,tub}^2 + \sigma_{v,sup}^2 + \sigma_{v,det}^2 \quad (1)$$

where $\sigma_{v,inj}^2$ is the peak variance induced by injection taking into account injected volume and mass, $\sigma_{v,tub}^2$ the variance induced by connection tubing between injector and column, column and suppressor, and suppressor and detector cell, $\sigma_{v,sup}^2$ the variance induced by the membrane suppressor, and $\sigma_{v,det}^2$ the variance induced by the detector cell. To assess the influence of injection parameters, volume- and mass-loadability contributions were systematically assessed using a system with minimal internal volume, using a low-capacity column packed with 2.5 µm particles, and considering dispersion characteristics of early-eluted ions (k between 0.1 and < 1.5). These experiments indicate that early eluted

compounds are negatively affected by volume overloading, all analytes experience the same dilution effect but the focusing effect is proportional to *k.* More retained compounds suffer mostly from mass overloading, as they are smeared out over a larger distance in the column due to a limited number of ion-exchange sites per unit length. Fig. 3A shows the effect of system configuration, considering tubing i.d. and the internal volumes of the suppressor and the detector cell, on resulting dispersion characteristics in terms of reduced plate height (black lines) and the total peak variance (red lines), respectively. Using a system configuration that encompasses a conventional suppressor with 15 µL internal volume and an analytical scale detector with an 0.7 µL flow cell and fitted with a 250 µm i.d. × 300 mm long inlet tubing (15 µL) and preheater with an internal volume of 10 µL, the separation performance was significantly degraded, even for late eluted ions (squares). When replacing the detector cell for a flow cell with an internal volume of only 20 nL and reducing the i.d. of the inlet tubing to 100 µm and length (L = 200 mm), and bypassing the preheater, the reduced plate heights were reduced by 40% for early eluted ions and 20% for late eluted ions respectively (triangles). Noise levels were determined to be comparable for both type of detectors (see SI for more information). Still, this configuration only provides acceptable performance for retained ions with k > 3. After applying a prototype suppressor module with an internal volume of only 7.5 µL that can effectively suppress mobile phases up to 60 mM at flow rates up to 400 µL/min corresponding to a capacity of 25 µEq./min, the best performance was achieved providing reduced plate-height values below 4 for ions with k > 1 and as low as h ~ 2 for k = 5 (circles). The system optimization allowed reduction of peak variance by 80% for early eluted analytes to 40% for late eluted ions. The performance improvement induced by the system configuration is illustrated in Fig. 3B (performance data listed in SI). Based on the difference in the position of water dip, it is estimated the 100 µL of dead volume has been removed from the post-column flow path with respect to the conventional configuration.

Thermal heating and effect of column wall. Percolation of a liquid through columns packed with 2.5 µm particles at ultra-high pressure induces frictional heating, which in turn

induces axial and radial temperature gradients over the column, affecting retention characteristics and/or efficiency. The extent of frictional heat created in 2 mm i.d. × 100 mm long SS column packed with 2.5 µm particles while operating the column close to the system pressure limit, applying F = 0.4 mL/min, was determined with thermocouples mounted on to the end fittings to be ΔT = 2.5 °C under forced-air conditions, and ΔT = 5.8 °C under still-air conditions. Using the novel column hardware, the temperature difference between column inlet and outlet at the exterior of the end fitting to be ΔT = 1.5 °C in the forced-air column oven and ΔT = 4.1 °C in the still-air column oven. It should be noted that the PEEK lining acts to some extent as an insulator (thermal conductivity of PEEK is 0.25 $W \cdot m^{-1} \cdot K^{-1}$ *versus* 16 $W \cdot m^{-1} \cdot K^{-1}$ for SS), reducing the heat exchange between the flow path and column exterior. As a result, the temperature of mobile phase flowing within the PEEK insulated flow path is higher and the chromatographic operating conditions approach near-adiabatic operation. The increase in temperature across the column length does lead to an increase in retention of late eluted ions, which contrasts with analyte retention behavior typically observed in RP-LC mode where retention generally decreases with temperature.[21,25] Fig. 4 shows overlays of chromatograms of ions separated on a 100 mm long PEEK lined column at 70 MPa applying forced-air (isothermal) column-oven configuration and still-air (adiabatic) column-oven configuration, respectively. In IC, the temperature increase leads to a decrease in the thickness of the hydration shell of water molecules present around the ions. This leads to an increase in entropy, and hence a decrease in Gibbs free energy, which in turn favors the interaction between ions and the stationary phase. This effect is more pronounced for analytes with a thin hydration shell, which are typically late eluted analytes, *i.e.,* analytes that are larger and exhibit a lower charge density. Additionally, the dependency of retention on temperature is different for monovalent and divalent ions, in part resulting from the differences in hydration energy, as is reflected by different slopes in a van ‘t Hoff plot (similar to a different dependency of retention on eluent strength in a selectivity plot). Under adiabatic conditions the separation efficiency was approximately 10% higher (124,000 /m *versus* 111,000 /m plates for the last

eluted analyte). In contrast, when heat is actively removed via the column wall, the radial temperature gradient becomes more pronounced which leads to the formation of a parabolic flow profile and corresponding increase in chromatographic dispersion. Such behavior is in agreement with what has been observed in reversed-phase under UHPLC conditions.[26-29]

Method speed-up and kinetic performance limits. The kinetic performance limits were assessed applying UHPIC conditions (70 MPa) and a still-air column-oven configuration. Fig. 5A shows van Deemter curves of conventional IC columns (4 µm SMP particles coated with 65 nm latex particles) in comparison with UHPIC column technology (2.5 µm SMP and MiP particles coated with 40 nm latex particles). As expected, when applying the same particle architecture, the increase in optimal flow velocity when applying 2.5 µm instead of 4 µm particle packed columns is proportional to the ratio of the particle diameters (a factor 1.6), and the plate height decreases proportional to the particle diameter. When applying the microporous 2.5 µm particles, the optimum flow velocity is further increased (1.3 to 2.1 mm/s) and minimum plate height decreases from 7.1 to 5.1 µm, corresponding to a reduced plate height of 2.1. Contributing to this value is the narrow particle size distribution for the MiP particles. Also, the morphology is very uniform compared to the super-macroporous particles (see Fig 1B). This combination results in a denser column packing, which also affects the column permeability (which is lower for the MiP particle-packed column compared to the SMP column packed with the same mode particle size). The kinetic performance limits, constructed from experimental van Deemter and column permeability ($K_{v,0}$) data [15,22] are compared in Fig. 5B. Ultra-high-pressure operation utilizing the UHPIC columns offers a significant time gain, while separation efficiency is not compromised, *e.g.*, when moving from 4 µm packed columns operated at 35 MPa to 2.5 µm particle columns operated at 70 MPa for N = 20,000, the analysis time is reduced with a factor (G_t) of 1.9 (employing same particle type) based on $G_t = t_{0\,(4\,\mu m;\,35\,MPa)} / t_{0\,(2.5\,\mu m;\,70\,MPa)}$. Representative chromatograms are depicted in Fig. 6. When using the 2.5 µm microporous particles while accordingly downscaling the nanobead diameter a kinetic time gain factor G_t of 3.4 was even achieved, which is attributed to the significantly

reduced *A*-term contribution. Fig. S2 shows free-length kinetic plots constructed using the data from Fig. 5, illustrating how column lengths may be altered to achieve a given plate number with the novel stationary phases and system.

CONCLUSIONS

The performance limits of a prototype ultra-high-pressure (70 MPa) IC instrument with suppressed conductivity in combination with columns packed with 2.5 µm anion-exchange particles have been successfully explored. After optimization of the configuration with respect to extra-column dispersion, reduced plate heights as low as 2.1 were achieved. The main source of extra-column dispersion is currently the suppressor module, in which a compromise is made between membrane contact area affecting suppression efficacy and the internal volume influencing dispersion characteristics. The novel column technology with PEEK flow path, compatible with corrosive solvents and high-pressure operation up to 150 MPa (during column packing), reduces the heat exchange between the flow path and the column-oven compartment. Still, by changing the column-oven configuration either (near) isothermal or adiabatic conditions can be reached. Hence, depending on the requirements, high-pressure method-transfer strategies can be pursued where selectivity is maintained using a forced-air oven, or where separation efficiency is maximized applying a still-air oven configuration. A kinetic time-gain factor of 2 have been established without compromising separation efficiency making use of the novel column formats and optimized high-pressure system. When the stationary phase architecture is altered, from super-macroporous to microporous, an additional gain in efficiency and/or analysis time can be established, enabling the sub-1-minute separation of fluoride, chlorite, chloride and nitrite using the 70 MPa pressure-rated system.

ACKNOWLEDGEMENTS

SW acknowledges the Flemish Agency for Innovation and Entrepreneurship and the Research Foundation Flanders (V408618N) for funding. JLDS and SE acknowledge the Research Foundation Flanders (FWO) for financial support (grant no. G025916N). Yury Agroskin, Kannan Srinivasan, Andrew Zill, Hongmin Zang, Zhongqing Lu, Anna Blank, and Sheetal Bhardwaj (Thermo Fisher Scientific) are acknowledged for their support.

CONFLICT OF INTEREST DISCLOSURE

The authors declare no competing financial interest.

REFERENCES

[1] Small, H.; Stevens, T.; Bauman, W.C., Novel ion exchange chromatographic method using conductometric detection. *Anal. Chem.* 1975, *47*, 1801-1809.

[2] Haddad, P.R.; Nesterenko, P.N.; Buchberger, W., Recent developments and emerging directions in ion chromatography. *J. Chromatogr. A* 2008*, 1184*, 456-473.

[3] Liu, Y.; Srinivasan, K.; Pohl, C.A.; Avdalovic, N., Recent developments in electrolytic devices for ion chromatography. *J. Biochem. Biophys. Methods* 2004, *60*, 205-232.

[4] Zatirakha, A.V.; Smolenkov, A.D.; Shpigun, O.A., Preparation and chromatographic performance of polymer-based anion exchangers for ion chromatography: a review. *Anal. Chim. Acta* 2016, *904*, 33-50.

[5] Wouters, S.; Haddad, P.R.; Eeltink, S., System design and emerging hardware technology for ion chromatography. *Chromatographia* 2017, *80*, 689-704.

[6] Popp, M.; Hann, S.; Mentler, A.; Fuerhacker, M.; Stingeder, G.; Koellensperger, G., Determination of glyphosate and AMPA in surface and waste water using high-performance ion chromatography coupled to inductively coupled plasma dynamic reaction cell mass spectrometry (HPIC-ICP-DRC-MS). *Anal. Bioanal. Chem.* 2008, *391*,695-699.

[7] Verrey, D.; Louyer, M.V.; Thomas, O.; Baures, E., Direct determination of trace-level haloacetic acids in drinking water by two-dimensional ion chromatography with suppressed conductivity. *Microchem. J.* 2013, *110*, 608-613.

[8] Tian, K.; Dasgupta, P.K.; Anderson, T.A., Determination of trace perchlorate in high-salinity water samples by ion chromatography with on-line preconcentration and preelution. *Anal. Chem.* 2003, *75*, 701-706.

[9] Lammarino, M.; Di Taranto, A.; Muscarella, M.; Nardiello, D.; Palermo, C.; Centonze, D., Development of a new analytical method for the determination of sulfites in fresh meats and shrimps by ion-exchange chromatography with conductivity detection. *Anal. Chim. Act*a 2010, *672*, 61-65.

[10] Palermo, C.; Muscarella, M.; Nardiello, D.; Lammarino, M.; Centonze, D., A multiresidual method based on ion-exchange chromatography with conductivity detection for the determination of biogenic amines in food and beverages. *Anal. Bioanal. Chem.* 2013, *405*, 1015-1023.

[11] Lu, Z.; Liu, Y.; Barreto, V.; Pohl, C.; Avdalovic, N.; Joyce, R.; Newton, B., Determination of anions at trace levels in power plant water samples by ion chromatography with electrolytic eluent generation and suppression. *J. Chromatogr. A* 2002, *956*,129-138.

[12] Živojinovic, D.Z.; Rajakovic, L.V., Application and validation of ion chromatography for the analysis of power plants water: Analysis of corrosive anions in conditioned water-steam cycles. *Desalination* 2011, *275*, 17-25.

[13] Macnair, J.E.; Lewis, K.C.; Jorgenson, J.W., Ultrahigh-pressure reversed-phase liquid chromatography in packed capillary columns. *Anal. Chem.* 1997, *69*, 983-989.

[14] Mazzeo, J.R.; Neue, U.D.; Kele, M.; Plumb R.S., Advancing LC performance with smaller particles and higher pressure. *Anal. Chem.* 2005, *77*, 460-467.

[15] De Vos, J.; De Pra, M.; Desmet, G.; Swart, R.; Edge, T.; Steiner, F.; Eeltink, S., High-speed isocratic and gradient liquid-chromatography separations at 1500 bar. *J. Chromatogr. A* 2015, *1409*, 138-145.

[16] Wouters, B.; Bruggink, C.; Desmet, G.; Agroskin, Y.; Pohl, C.A.; Eeltink, S., Capillary ion chromatography at high pressure and temperature. *Anal. Chem.* 2012, *84*, 7212-7217.

[17] Lucy, C.A.; Wahab, M.F., Advances in high-speed and high resolution ion chromatography. *LGGC* 2013, *31*, 38-42.

[18] Wahab, M.F.; Pohl, C.A.; Lucy, C.A., Colloidal aspects and packing behaviour of charged microparticulates in high efficiency ion chromatography. *J. Chromatogr. A* 2012, *1270,* 139-146.

[19] Shellie, R.A.; Tyrrell, E.; Pohl, C.A.; Haddad P.R., Column selection for comprehensive multidimensional ion chromatography. *J. Sep. Sci.* 2008, *31*, 3287-3296.

[20] Desmet, G.; Clicq, D.; Gzil, P., Geometry-independent plate height representation methods for the direct comparison of the kinetic performance of LC supports with a different size or morphology. *Anal. Chem.* 2005, *77*, 4058-4070.

[21] Cabooter, D.; Heinisch, S.; Rocca, J.L.; Clicq, D.; Desmet, G., Use of the kinetic plot method to analyze commercial high-temperature liquid chromatography systems: I: Intrinsic performance comparison. *J. Chromatogr. A* 2007, *1143*, 121-133.

[22] De Vos, J.; Broeckhoven, K.; Eeltink, S., Advances in ultrahigh-pressure liquid chromatography technology and system design. *Anal. Chem.* 2015, *88*, 262-278.

[23] Strong, D.L.; Ung, J.C.; Dasgupta, P.K., Electrodialytic eluent generation and suppression: ultralow background conductance suppression anion chromatography. *J. Chromatogr.* 1991, *546,* 159-173.

[24] Yang, G.; Takeuchi, M.; Dasgupta, P.K., On-line gas-free electrodialytic eluent generator for capillary ion chromatography. *Anal. Chem.* 2008, *80*, 40-47.

[25] Wouters, B.; Bruggink, C.; Desmet G.; Agroskin, Y.; Pohl, C.A., Eeltink S. Capillary ion chromatography at high pressure and temperature. *Anal. Chem.* 2012, *84*, 7212-7217.

[26] Broeckhoven, K.; Billen, J.; Verstraeten, M.; Choikhet, K.; Dittmann, M.; Rozing, G.; Desmet, G., Towards a solution for viscous heating in ultra-high pressure liquid chromatography using intermediate cooling. *J. Chromatogr. A* 2010, *1217*, 2022-2031.

[27] Gritti, F.; Martin, M.; Guiochon, G., Influence of viscous friction heating on the efficiency of columns operated under very high pressures. *Anal. Chem. 2009*, 81, 3365-3384.

[28] Gritti, F.; Guiochon, G., Consequences of the radial heterogeneity of the column temperature at high mobile phase velocity. *J. Chromatogr. A 2007*, 1166, 47-60.

[29] de Villiers, A.; Lauer, H.; Szucs, R.; Goodall, S.; Sandra, P. Influence of frictional heating on temperature gradients in ultra-high-pressure liquid chromatography on 2.1 mm ID columns. *J. Chromatogr. A* 2006, *1113*, 84-91.

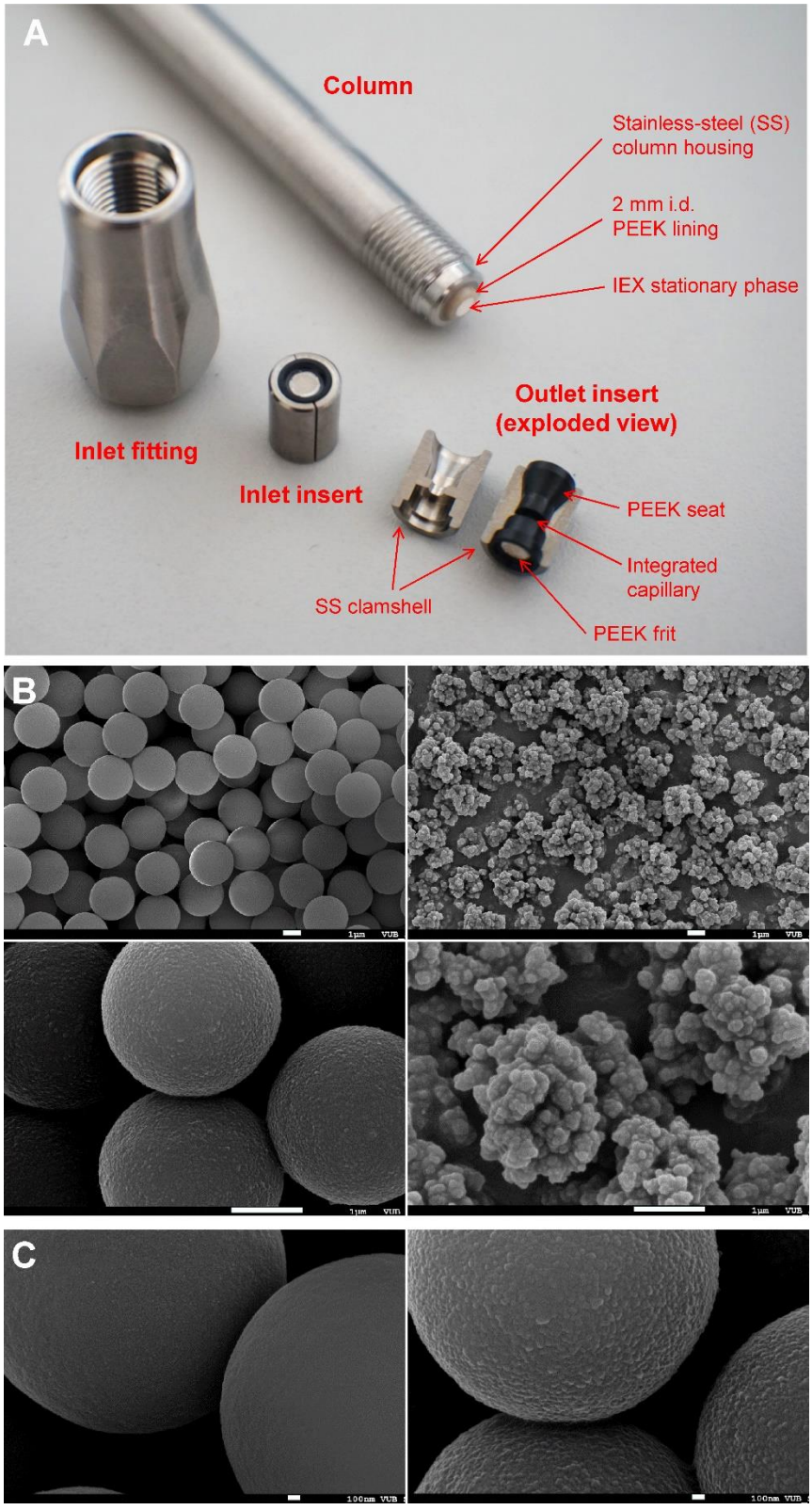

Figure 1. (A) Disassembled prototype column compatible with corrosive solvents showing the PEEK lining and special inserts for inlet and outlet fitting. The insert comprises of a PEEK seat integrated with a frit, fixed in a stainless-steel clamshell cartridge. (B) SEM of microporous

(left) and super-macroporous 2.5 µm particles (right) at different magnifications, (C) comparison of bare particles (left) and coated microporous 2.5 µm particles coated with nanobeads extracted from an IC column after use (right).

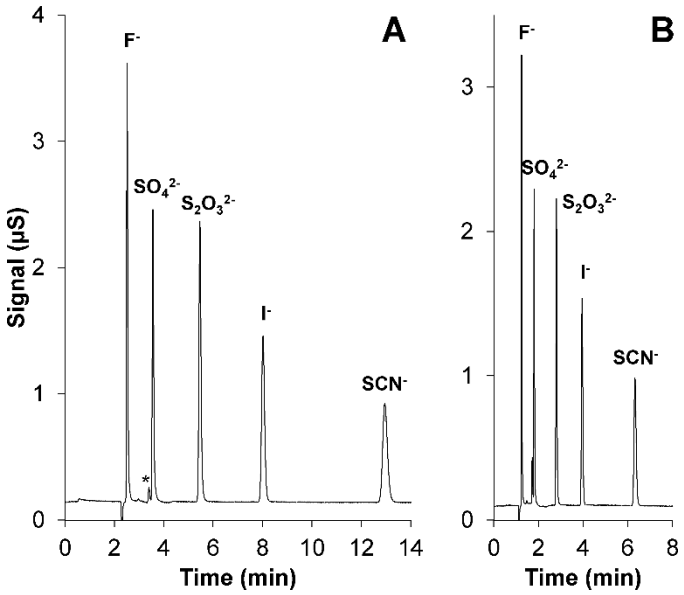

Figure 2. Isocratic separations of small inorganic anions on a 150 mm long column packed with 2.5 µm-SMP particles operated at (A) its optimal flow velocity (u_{opt} = 130 µL/min, ΔP = 38 MPa), and (B) at the kinetic performance limit of 70 MPa using a fully-optimized UHPIC system with respect to extra-column dispersion (*vide infra*). The water dip represents the t_0 marker and * is the impurity carbonate. The eluent concentration was 35 mM KOH.

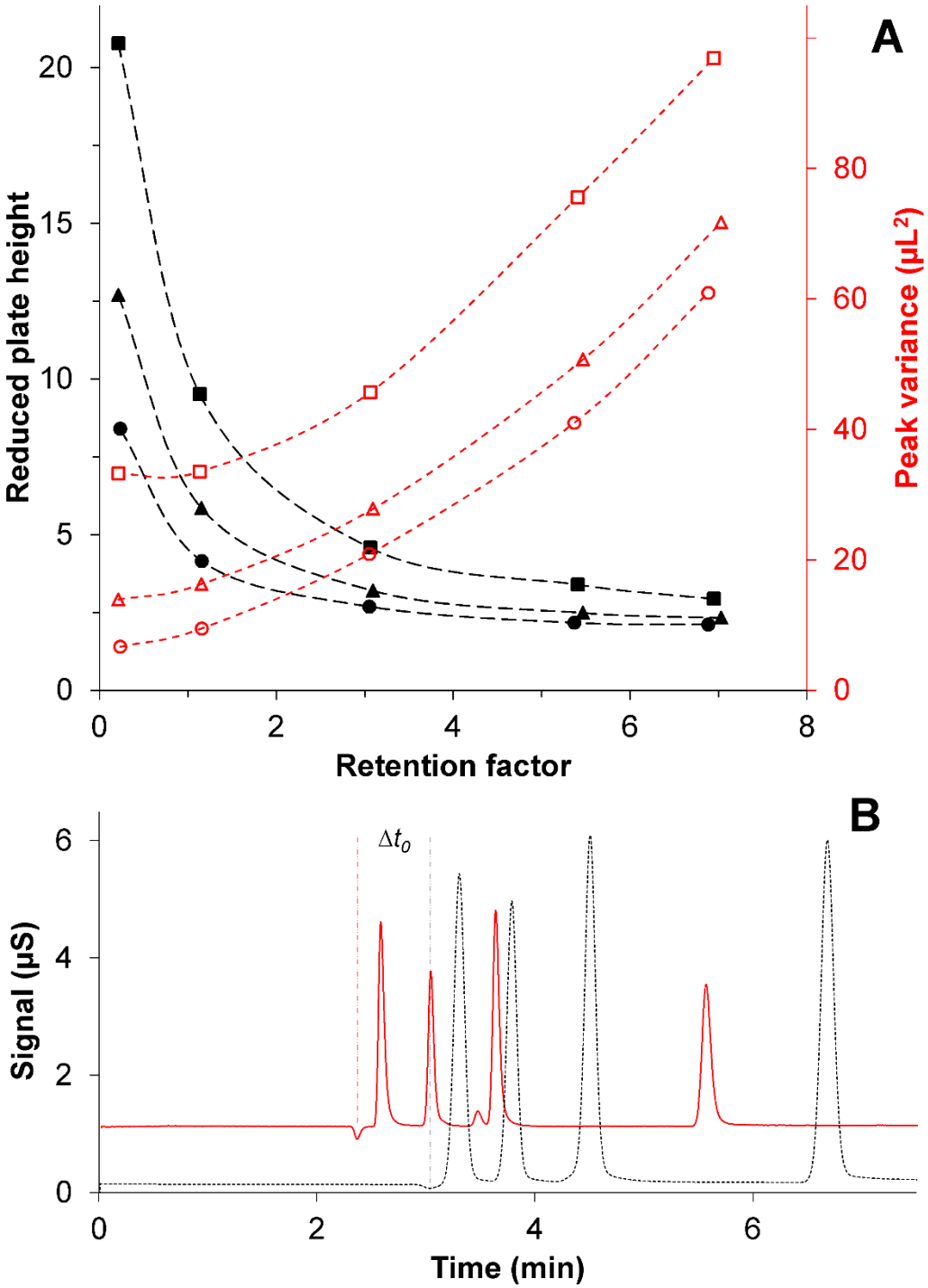

Figure 3. (A) Reduced plate-height values (black lines) and corresponding volumetric variances (red lines) for 5 inorganic anions determined using different system configurations: (■) 15 µL suppressor + analytical detector with 250 µm i.d. inlet tubing, a preheater, and 0.7 µL cell, (▲) 15 µL suppressor + capillary detector with 100 µm i.d. inlet tubing and 20 nL cell, (●) 7.5 µL suppressor + capillary detector. (B) Chromatograms illustrating the performance of inorganic anions (F^-, SO_4^{2-}, $S_2O_3^{2-}$, I^-) on a column packed with 2.5 µm SMP particles using a

conventional ICS5000 system (dotted black) and using a fully optimized UHPIC system with reduced dispersion (solid red), respectively. The eluent concentration was 23 mM KOH.

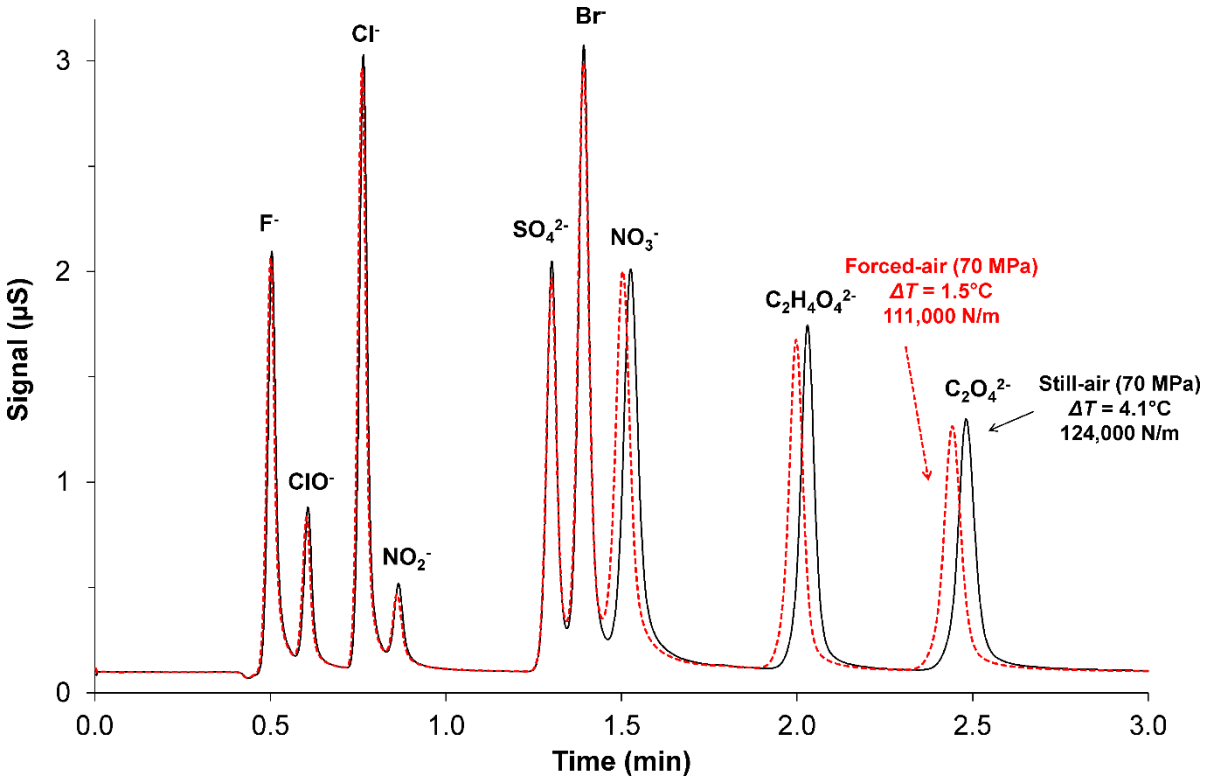

Figure 4. Overlay of the separation of a mixture of mono- and divalent ions a 100 mm long column operated at 70 MPa (*F* = 400 µL/min) at 30.0°C while maintaining near adiabatic conditions (dotted line) applying a forced-air column oven configuration and near isothermal conditions (solid line) applying a still-air column oven configuration. Other conditions similar as in Fig 2.

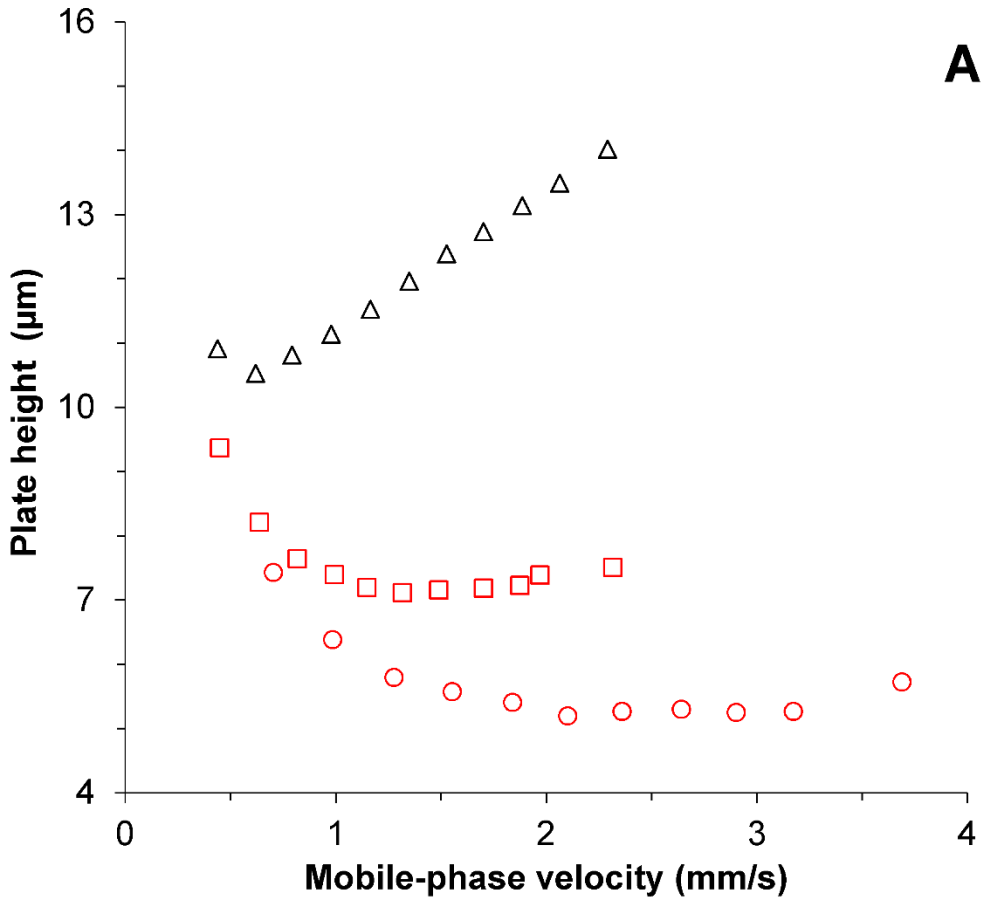
A
16
13
10
7
4
0
1
2
3
4
Plate height (µm)
Mobile-phase velocity (mm/s)

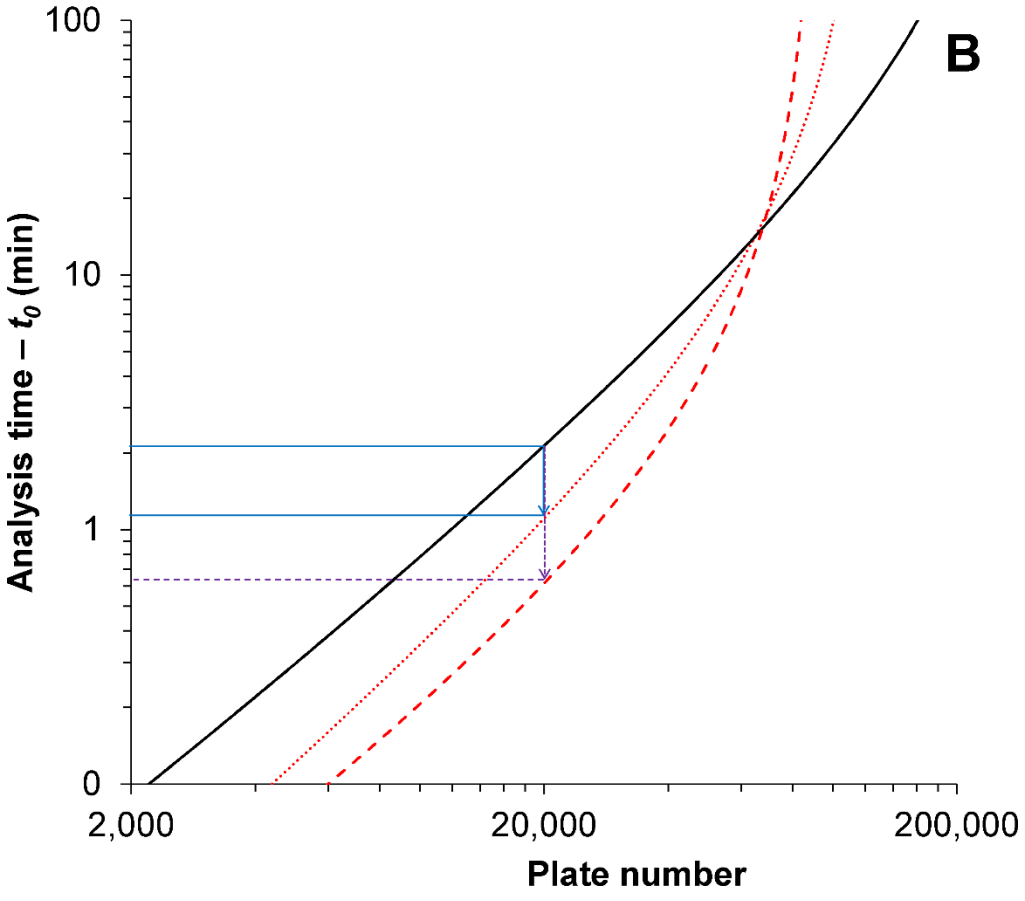
B
100
10
1
0
2,000
20,000
200,000
Analysis time – t_0 (min)
Plate number

Figure 5. Performance assessment using the classical van Deemter curve (A) and kinetic plots (B) operating the column with 4 µm SMP particles (Δ, black solid line) at a maximum pressure of 35 MPa and the columns packed with 2.5 µm SMP particles (□, red dotted line) and 2.5 µm MiP particles (○, red dashed line) at a maximum pressure of 70 MPa and near isothermal conditions. Other conditions similar as in Fig 2. The solid blue arrow depicts a time gain factor of 1.9 (maintaining 20,000 plates). A time gain factor of 3.4 characterized by purple dotted arrow is obtained when moving from 4 µm particles to 2.5 µm microporous particles and raising the pressure limits.

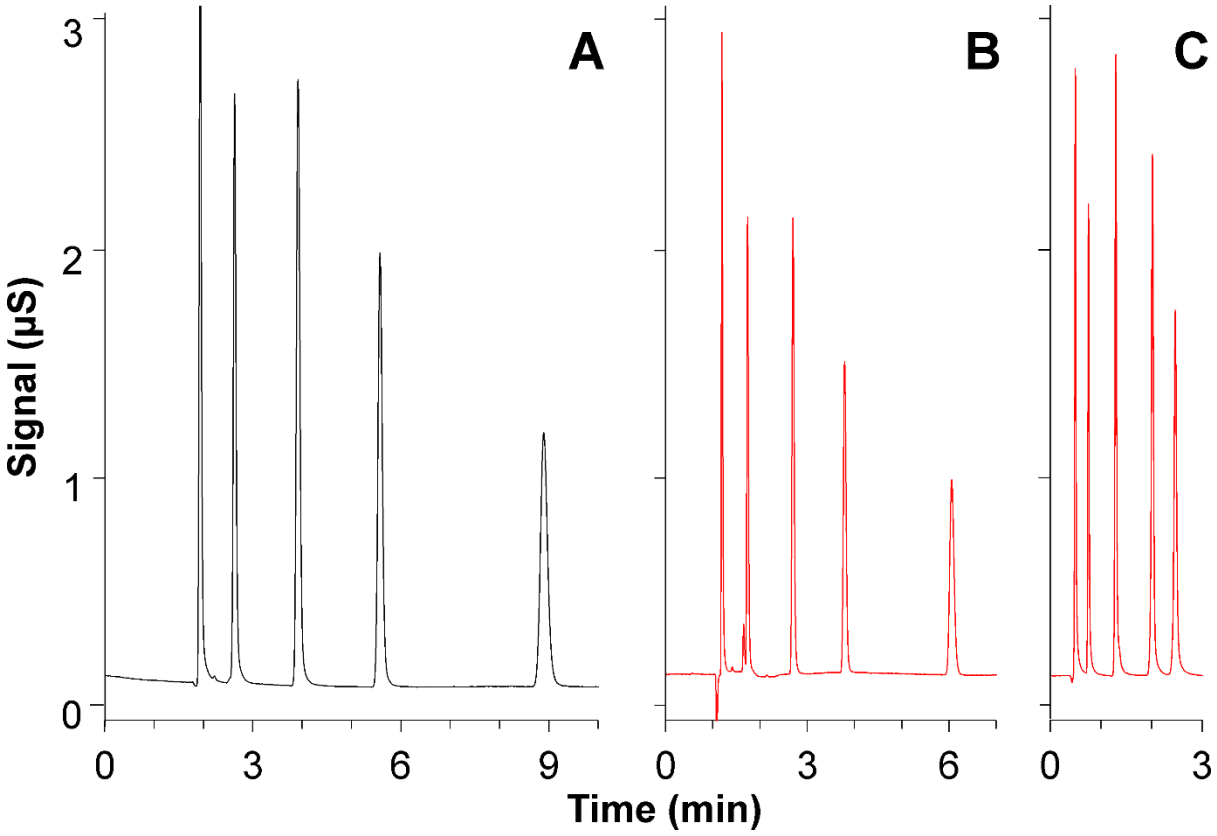

Figure 6. Chromatograms of anions (F^-, SO_4^{2-}, $S_2O_3^{2-}$, I^-, SCN^-) recorded close to the kinetic performance limits of (A) 35 MPa on a 250 mm long column packed with 4 µm SMP particles, (B) 70 MPa on a 150 mm long column packed with 2.5 µm SMP particles, and (C) 70 MPa on a 150 mm long column packed with 2.5 µm MiP particles.